Model-Based Characterization of the Bidirectional Interaction Between Pharmacokinetics and Tumor Growth Dynamics in Patients with Metastatic Merkel Cell Carcinoma Treated with Avelumab

Ana-Marija Grisic[1], Wenyuan Xiong[2], Lénaïg Tanneau[3], Siv Jönsson[3], Lena E. Friberg[3], Mats O. Karlsson[3], Haiqing Dai[4], Jenny Zheng[5], Pascal Girard[2], and Akash Khandelwal[1]

ABSTRACT

Purpose: Empirical time-varying clearance models have been reported for several immune checkpoint inhibitors, including avelumab (anti–programmed death ligand 1). To investigate the exposure-response relationship for avelumab, we explored semimechanistic pharmacokinetic (PK)–tumor growth dynamics (TGD) models.

Patients and Methods: Plasma PK data were pooled from three phase I and II trials (JAVELIN Merkel 200, JAVELIN Solid Tumor, and JAVELIN Solid Tumor JPN); tumor size (TS) data were collected from patients with metastatic Merkel cell carcinoma (mMCC) enrolled in JAVELIN Merkel 200. A PK model was developed first, followed by TGD modeling to investigate interactions between avelumab exposure and TGD. A PK-TGD feedback loop was evaluated with simultaneous fitting of the PK and TGD models.

Results: In total, 1,835 PK observations and 338 TS observations were collected from 147 patients. In the final PK-TGD model, which

included the bidirectional relationship between PK and TGD, avelumab PK was described by a two-compartment model with a positive association between clearance and longitudinal TS, with no additional empirical time-varying clearance identified. TGD was described by first-order tumor growth/shrinkage rates, with the tumor shrinkage rate decreasing exponentially over time; the exponential time-decay constant decreased with increasing drug concentration, representing the treatment effect through tumor shrinkage inhibition.

Conclusions: We developed a TGD model that mechanistically captures the prevention of loss of antitumor immunity (i.e., T-cell suppression in the tumor microenvironment) by avelumab, and a bidirectional interaction between PK and TGD in patients with mMCC treated with avelumab, thus mechanistically describing previously reported time variance of avelumab elimination.

Introduction

Merkel cell carcinoma (MCC), a rare and aggressive neuroendocrine skin tumor, is associated with UV exposure, advanced age, and clonal integration of the Merkel cell polyomavirus (1). MCC can metastasize early, and patients with metastatic disease have limited treatment options; median survival with chemotherapy is <10 months (2, 3).

Immune checkpoint inhibitors, including anti–programmed death 1 (PD-1) and anti–programmed death ligand 1 (PD-L1) mAbs, are effective treatments for a wide range of tumor types (4–8). Within this

class, avelumab is a fully human anti–PD-L1 immunoglobulin G1 (IgG1) mAb. In 2015, avelumab received breakthrough, fast-track, and orphan drug designations from the FDA for the treatment of metastatic MCC (mMCC). In part A of the pivotal phase II JAVELIN Merkel 200 trial (NCT02155647), performed in 88 patients with mMCC whose disease had progressed after ≥1 line of chemotherapy, avelumab treatment resulted in an objective response rate of 31.8% (9). In 2017, avelumab became the first approved treatment for mMCC based on these data. Avelumab is now also approved in various countries worldwide as monotherapy for locally advanced or metastatic urothelial carcinoma (first-line maintenance or second-line treatment) and in combination with axitinib for the first-line treatment of advanced renal cell carcinoma (10, 11). Avelumab binds to PD-L1 on tumor cells, preventing its binding to PD-1 on T cells and subsequent suppression and inactivation of T-cell–mediated immune responses (12). Avelumab is also the first approved anti–PD-L1 antibody containing a wild-type IgG1 Fc region, which has been shown in preclinical studies to induce antibody-dependent cell-mediated cytotoxicity (ADCC) by binding to the Fc-gamma receptor (FcγR) of natural killer cells, providing an alternative mechanism for inducing immunogenic tumor cell death (12, 13).

Main clearance (CL) pathways of mAbs include unspecific (through binding of mAb Fc region to FcγR-expressing cells) and specific (through binding of mAb Fab region to the specific mAb target, i.e., target-mediated drug disposition) endocytosis, followed by intracellular catabolism through lysosomal degradation (14, 15). The CL of mAbs, including immune checkpoint inhibitors such as avelumab, has been reported to decrease during treatment (16, 17). In patients with mMCC (N = 88), the mean maximum change in avelumab CL was 32.1% (17). The reduction in CL over time was greater in patients who

[1]the healthcare business of Merck KGaA, Darmstadt, Germany. [2]Merck Institute of Pharmacometrics, Lausanne, Switzerland, an affiliate of Merck KGaA, Darmstadt, Germany. [3]Department of Pharmacy, Uppsala University, Uppsala, Sweden. [4]EMD Serono, Billerica, Massachusetts. [5]Pfizer, Inc., La Jolla, California.

Note: Supplementary data for this article are available at Clinical Cancer Research Online (http://clincancerres.aacrjournals.org/).

A.-M. Grisic and W. Xiong contributed equally as co-first authors of this article.

Current address for W. Xiong: UCB, Bulle, Switzerland.

Corresponding Author: Akash Khandelwal, the healthcare business of Merck KGaA, Frankfurter Str. 250, Darmstadt 64293, Germany. Phone: 4961-5172-43323; Fax: 4961-5172-56684; E-mail: akash.khandelwal@merckgroup.com

Translational Relevance

Immune checkpoint inhibitors, including avelumab (anti–PD-L1), are effective treatments for various tumors. Clearance of immune checkpoint inhibitors has been reported to be time-varying and to decrease during treatment, leading to a biased steep estimate of the exposure-efficacy relationship. We developed a joint pharmacokinetic (PK)–tumor size model of avelumab to characterize the bidirectional interaction between avelumab exposure and tumor growth dynamics (TGD) using plasma concentration and tumor size observations from patients with metastatic Merkel cell carcinoma (mMCC). We observed an exposure-dependent treatment effect of avelumab in slowing the decay of tumor shrinkage, with avelumab clearance positively associated with tumor size. To our knowledge, we report the first model characterizing the bidirectional interaction between plasma drug concentration and tumor growth dynamics for an immune check-point inhibitor. Our model captures the mechanistic effect of avelumab of relieving T cells from immunosuppression and restoring antitumor immune responses and may help to inform future clinical studies.

responded to treatment (17), potentially due to the resulting tumor shrinkage and decreased antigen (PD-L1) burden. This finding implies that the standard exposure-response relationship (which suggested that greater exposure may be associated with an increased probability of objective response in patients with mMCC) was confounded due to the bidirectional effect of exposure/CL and tumor size/response. This interaction between treatment effect and drug exposure may lead to a biased steeper estimate of the exposure-efficacy relationship (18). We hypothesized that including avelumab CL as a function of longitudinal tumor size (TS) in a joint pharmacokinetics (PK)–tumor growth dynamics (TGD) analysis may account for observed time-varying CL with mAbs, and characterization of the bidirectional interaction between PK and TGD could potentially provide an unbiased estimation of the exposure-response relationship (19).

Here, we developed a joint PK-TGD model of avelumab based on data from patients with mMCC and evaluated the impact of the FcγR genotype on PK and TS.

Patients and Methods

Modeling data set

TS data from part A of the JAVELIN Merkel 200 trial (9) were evaluated in the analysis. The corresponding sparse-sampled plasma PK data from JAVELIN Merkel 200 were pooled with rich-sampled PK data from the JAVELIN Solid Tumor (NCT01772004) and JAVELIN Solid Tumor JPN (NCT01943461) trials to better characterize the PK of avelumab.

Study design and assessments

Study designs and eligibility criteria have been reported in detail previously (9, 12, 20). In part A of the phase II JAVELIN Merkel 200 trial, patients with mMCC who had received prior chemotherapy were treated with avelumab 10 mg/kg every 2 weeks (9). In the phase I JAVELIN Solid Tumor (12) and JAVELIN Solid Tumor JPN (20) trials, patients with metastatic or locally advanced solid tumors received avelumab at various doses in the initial dose-

escalation part, as outlined in Supplementary Table S1. The trials were conducted in accordance with the Declaration of Helsinki and the International Council on Harmonisation Guidelines on Good Clinical Practice, and the protocols were approved by the independent ethics committee or institutional review board at each participating center. All patients provided written informed consent before enrollment.

TS assessments were performed every 6 weeks (JAVELIN Solid Tumor JPN) or every 6 weeks for the first 12 months then every 12 weeks thereafter (JAVELIN Merkel 200 and JAVELIN Solid Tumor). TS was determined using the sum of longest diameters of target lesions per Response Evaluation Criteria in Solid Tumors (RECIST) version 1.1. PK sampling schedules by trial are provided in Supplementary Table S1.

PK-TGD model development

A sequential approach was applied in the model development. A PK model was established as the first step, followed by TGD modeling to test the effect of avelumab exposure on TGD. Thereafter, a feedback loop from TGD to the PK model was evaluated with simultaneously fitting of the PK and TGD models.

Plasma PK data were fitted with a prior structural PK model, which included a two-compartment model and first-order elimination (21). For the TGD model development, the model by Claret and colleagues was tested as a starting point, which assumes first-order tumor growth and first-order tumor shrinkage (22). Subsequently, a resistance model of tumor inhibition was tested, which assumes a time-dependent exponential decay of the tumor shrinkage rate (K_D; ref. 22). An exposure-dependent treatment effect was tested on the following parameters: tumor shrinkage rate K_D, effect decay (λ in **Fig. 1**), and simultaneously, both tumor shrinkage rate K_D and effect decay λ. Non-Gaussian distribution of baseline TS and effect decay required the use of Box-Cox transformation of random effects associated with these two parameters, and inclusion of between-patient variability in the residual error was needed as suggested by the assumption assessment of the model tested in qa Perl-speaks-NONMEM (PsN) functionality (23). Furthermore, the effects of albumin and longitudinal TS on CL were assessed as part of structural model development. Subsequently, we investigated
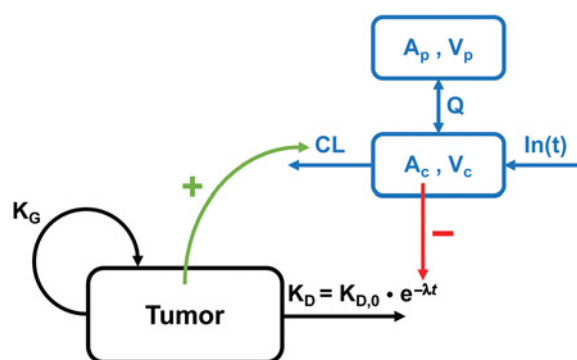
Figure 1.
Schematic representation of the final pharmacokinetics–tumor size model. Positive (+) and negative (−) associations are indicated. A_c, avelumab concentration in the central compartment; A_p, avelumab concentration in peripheral compartment; CL, avelumab clearance; K_D, tumor shrinkage rate; $K_{D,0}$, baseline tumor shrinkage rate; K_G, tumor growth rate; Q, intercompartmental exchange; t, time; V_c, avelumab central volume of distribution; V_p, avelumab peripheral volume of distribution; λ, exponential effect decay constant.

whether time variance in CL, previously reported for avelumab (17), could still be identified after accounting for the bidirectionality of PK-TS relationship by including the effect of TS on CL. Finally, covariate investigations were performed on the established PK-TGD model, whereby preselected covariates were assessed via forward selection and backward elimination based on statistical significance ($P < 0.01$), extent of the effect, and reduction of interindividual variability. The investigated covariates included age, body weight, lactate dehydrogenase, hemoglobin, estimated glomerular filtration rate [calculated according to Modification of Diet in Renal Disease (MDRD) formula], albumin, C-reactive protein, PD-L1 expression in tumor cells, number of nontarget lesions, sex, race, Eastern Cooperative Oncology Group performance status, and number of prior anticancer drug therapies. All covariates were explored on K_D, tumor growth rate (K_G), baseline TS, and effect decay. For CL and avelumab central volume of distribution (V_c), age, body weight, sex, race, and estimated glomerular filtration rate were explored.

Need for refinement for the stochastic models was assessed using the PsN functionality (23). The software package NONMEM (version 7.3.0) was used in the analysis. The first-order conditional estimation method with interaction (FOCEI) was used for the PK-TGD modeling. NONMEM runs on the servers were organized by PsN (version 4.4.8). The statistical software R (version 3.5.1) was used for the exploratory analysis and postprocessing of NON-MEM output.

To assess the relevance of the developed modeling approach, this model was compared with the traditional model (without effect of TS on CL, and thus without bidirectionality in the PK-TS relationship). To this end, using the stochastic simulation and estimation (SSE) procedure (automated in PsN), 500 data sets were simulated using the final (reference) model (including the bidirectional relationship), and subsequently the reference model and the traditional model that excludes the effect of TS on avelumab CL were fitted to the simulated data sets. Based on these estimations, relative root-mean-square error (RMSE) and relative bias were calculated as measures of accuracy and bias, respectively, and compared.

PK-TGD model qualification and dropout consideration

Models were evaluated by standard criteria, including objective function, goodness-of-fit plots, uncertainty of parameter estimation, and plausibility of parameter estimates. The predictive performance of the PK model was also assessed using prediction-corrected visual predictive checks (VPCs), in which 95% CIs were derived from 500 simulated data sets and compared with observed data. A dropout model was established to perform adequate VPCs for evaluation of the TGD model to correct the informative dropout-related bias in TS simulations. Because the dropout was not random and could be driven by disease progression or intolerability/toxicity (the former of which is clearly associated with TGD), a dropout model was required. A logistic regression modeling approach was chosen (24) rather than a survival analysis, given that dropout from TS assessment could only happen at the time of a visit and not randomly during the study. Dropout was assumed to occur at the time of the next planned tumor assessment following the last avelumab dose. Predictors selected *a priori* were added linearly in the logistic regression model.

Exploratory analysis of FcγR SNPs

Specific SNP genotypes were detected using TaqMan genotyping assays. A standalone 384-well PCR thermal cycler was used for amplification, and results were read on the Viia7 qPCR instrument. Genotyping assays specific for FcγRIIIA$_{158V}$ (rs396991) and FcγRIIA$_{131H}$ (rs1801274) were tested for each sample in duplicate. Each run included samples with known genotypes and a no template control lacking DNA template. Genotype calling for each assay was conducted using the Viia7 software (version 1.2.1). The raw output file created by this software was used to assign final genotypes. In an exploratory analysis, percentage TS change from baseline in Fcγ genotype patient subgroups was compared using spider plots. The distribution of random-effect parameters obtained from the PK-TGD model was also inspected against the Fcγ genotypes. If graphical analysis results suggested any association between the genotype and TS profile or TGD metrics, the impact of Fcγ polymorphism would be quantified by including it as a covariate in the TGD model.

Data availability statement

Any requests for data by qualified scientific and medical researchers for legitimate research purposes will be subject to the Data Sharing Policy of the healthcare business of Merck KGaA. All requests should be submitted in writing to the data sharing portal of the healthcare business of Merck KGaA (https://www.merckgroup.com/en/research/our-approach-to-research-and-development/healthcare/clinical-trials/commitment-responsible-data-sharing.html). When the healthcare business of Merck KGaA has a coresearch, codevelopment, or comarketing or copromotion agreement, or when the product has been out-licensed, the responsibility for disclosure might be dependent on the agreement between parties. Under these circumstances, the healthcare business of Merck KGaA will endeavor to gain agreement to share data in response to requests.

Results

Model data set

A total of 1,835 PK observations and 338 TS observations were available for analysis from 147 patients, including 53 patients enrolled in JAVELIN Solid Tumor (877 PK observations), 17 patients enrolled in JAVELIN Solid Tumor JPN (314 PK observations), and 77 patients enrolled in JAVELIN Merkel 200 (644 PK and 338 TS observations). The median number of PK and TS observations per patient was 14 (range, 1–24) and 3 (range, 1–13), respectively.

Final PK-TGD model

In the final model (**Fig. 1**), avelumab PK was described by a two-compartment model with TS-dependent CL. The only covariate included was baseline albumin level, which was found to be inversely related to CL. None of the other covariates had a significant effect on CL, V_c, or tumor-specific parameters. TGD was described by a first-order growth rate and a first-order shrinkage rate, with exponential effect decay that declines with time and drug concentration. TS was found to be linearly related to CL, with larger TS associated with higher CL. No additional empirical time variance of avelumab CL was identified. Alternative mathematical implementations were explored, including a power model for effect of TS on CL (seen in other tumors) and effect of drug exposure on K_D, but these had inferior performance. Implementing the effect of drug exposure on K_D alone or in addition to the exponential effect decay constant of K_D over time (λ) resulted in worse goodness-of-fit and implausible parameter estimates.

Table 1. Final model parameter estimates.

Parameter	Mean	Shrinkage (%)	Median (90% CI)[a]
Baseline TS, mm	93.5	—	85.9 (44.8–150)
K_D, month^{-1}	0.105	—	0.161 (0.102–0.363)
K_G, month^{-1}	0.0321	—	0.0275 (0.00372–0.0641)
λ, month^{-1}	0.199	—	0.193 (0.0479–0.465)
Effect of drug concentration on effect decay (Exposure$_{effect}$), 1/(µg/mL)	0.00052	—	0.00052 (0.0000125–0.00061)
CL, L/h	0.0236	—	0.252 (0.0194–0.0353)
V_c, L	3.29	—	3.28 (2.97–4.15)
Q, L/h	0.022	—	0.022 (0.0156–0.0270)
V_p, L	1.1	—	1.1 (0.836–1.52)
Effect of albumin on CL (Alb$_{effect}$), L/h per g/L albumin different from 40 g/L	−0.0193	—	−0.0184 (−0.0396 to −0.0131)
Effect of TS on CL (TS$_{effect}$), L/h per mm TS different from median TS 51 mm	0.00476	—	0.00486 (0.00243–0.00985)
Box-Cox for baseline TS	−0.391	—	−0.551 (−2.45–0.443)
Box-Cox for effect decay	−2.97	—	−2.97 (−2.99 to −2.97)
IIV of effect decay, variance	0.415	53	0.452 (0.137–51.6)
IIV of K_D, % CV	171	28	235 (93.0–479)
IIV of K_G, % CV	63	44	109 (21.1–404)
IIV of CL, % CV	31	14	31.3 (26.7–45.9)
IIV of V_c, % CV	25	9	26.2 (19.8–34.2)
IIV of baseline TS, variance	0.483	14	0.488 (0.128–1.40)
IIV of TS RUV, % CV	59	15	111 (33.0–210)
IIV of PK RUV, % CV	54	4	50.6 (38.7–69.7)
RUV PK (proportional error), % CV	13.9		13.7 (10.7–16.2)
RUV PK (additive error), ug/mL	2.55		2.42 (0.573–5.53)
RUV TS (proportional error), % CV	19.6		30.1 (19.1–482)
RUV TS (additive error), mm	0.0113		0.00011 (0.000113–0.0107)
Dropout: Intercept logit	−2.03 (fixed)		
Dropout: Effect of progressive disease	1.91 (fixed)		
Dropout: Effect of relative change from baseline TS	1.76 (fixed)		

Abbreviations: CL, avelumab clearance; CV, coefficient of variation; IIV, interindividual variability; K_D, tumor shrinkage rate; K_G, tumor growth rate; OFV, objective function; PK, pharmacokinetic; Q, intercompartmental exchange; RUV, residual unexplained variability; V_c, avelumab central volume of distribution; V_p, avelumab peripheral volume of distribution; λ, exponential effect decay constant over time.
[a]Bootstrap estimate ($n = 500$).

The final joint PK-TGD model (**Table 1**) is described by the following differential equations:

$$\frac{dA_c}{dt} = -\frac{CL \cdot TS_{effect} \cdot Alb_{effect}}{V_c} \cdot A_c - \frac{Q}{V_c} \cdot A_c + \frac{Q}{V_p} \cdot A_p$$

$$TS_{effect} = \left(1 + TS_{CL} \cdot \left(TS - TS_{baseline,median}\right)\right)$$

$$Alb_{effect} = \left(1 + Alb_{CL} \cdot \left(Alb_{baseline} - Alb_{baseline,median}\right)\right)$$

$$\frac{dA_p}{dt} = -\frac{Q}{V_p} \cdot A_p + \frac{Q}{V_c} \cdot A_c$$

$$\frac{dTS}{dt} = K_G \cdot TS - K_D \cdot TS \cdot e^{-\lambda \cdot t}$$

$$\lambda = \lambda_0 \cdot \left(1 - Exposure_{effect} \cdot \frac{A_c}{V_c}\right)$$

where A_c represents avelumab amount in the central compartment; $Alb_{baseline}$ represents baseline serum albumin level; $Alb_{baseline,median}$ represents median baseline serum albumin level; Alb_{CL} represents fractional change in CL with each g/L unit change in baseline albumin from median baseline albumin; Alb_{effect} represents the function describing albumin effect on CL; A_p represents avelumab amount in the peripheral compartment; CL represents avelumab clearance; $Exposure_{effect}$ represents effect of drug concentration on effect decay;

K_D represents tumor shrinkage rate; K_G represents tumor growth rate; TS represents tumor size (calculated as the sum of the longest diameter of the target lesions); $TS_{baseline}$ represents baseline tumor size; TS_{effect} represents the function describing tumor size effect on CL; Q represents avelumab intercompartmental clearance; V_c represents avelumab central volume of distribution; V_p represents avelumab peripheral volume of distribution; and λ represents the exponential decay constant of K_D over time.
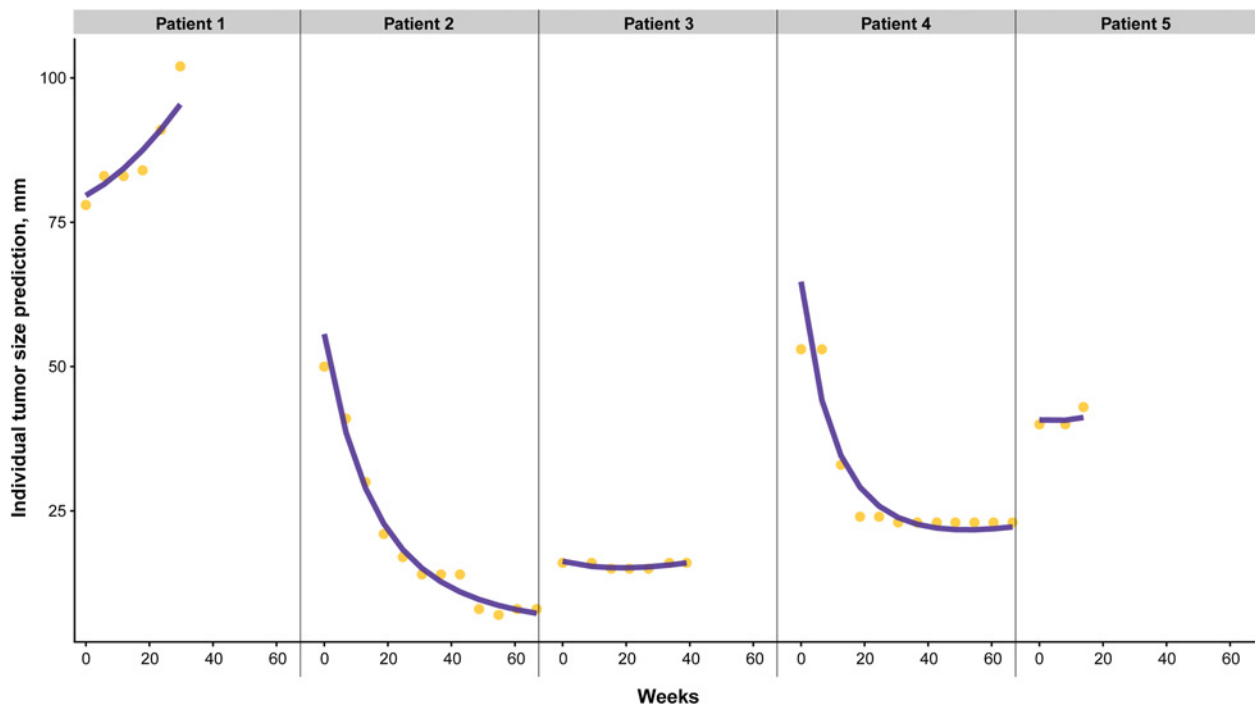
Dropout model

A logistic regression dropout model, consisting of a linear function of predictors that relate to TS measurement, was used to describe the probability of dropout at a visit. The predictors included in the final dropout model were relative change from baseline TS and progressive disease (defined as ≥20% TS increase from nadir with a minimum absolute 5-mm increase, per RECIST 1.1; ref. 25).

$$LP = \theta_0 + \theta_{CBTS} \cdot CBTS + \theta_{PRD} \cdot PD$$

$$\mu = \frac{e^{LP}}{1 + e^{LP}}$$

where CBTS represents relative change from baseline TS; LP represents linear function of predefined informative predictors; PD represents progressive disease [yes/no; (1/0)]; and μ represents probability of dropout at a visit.
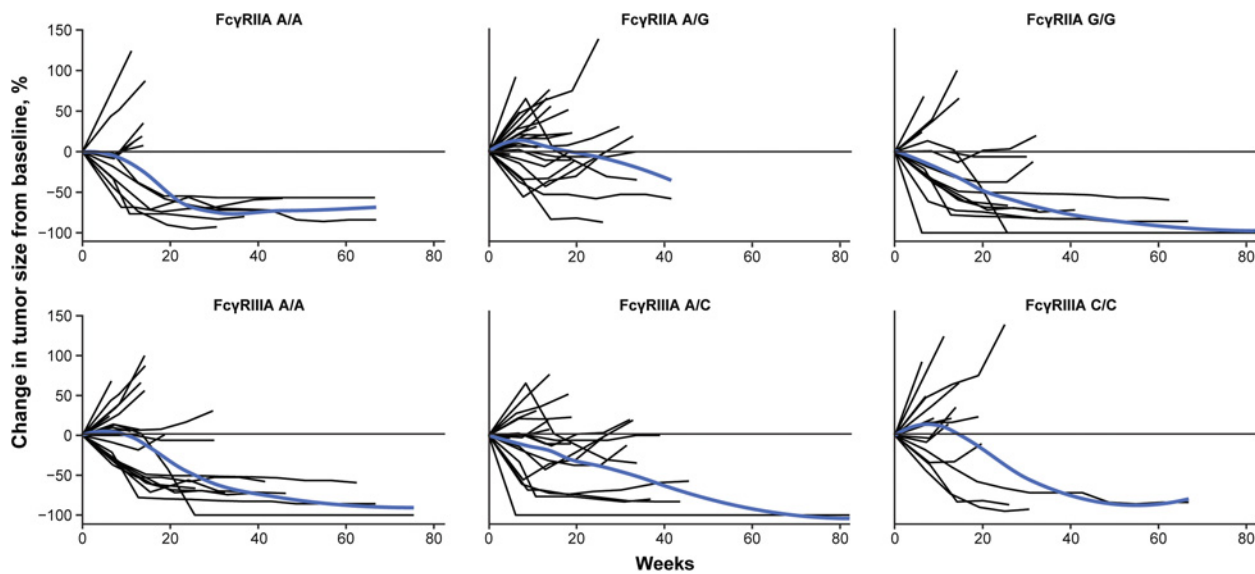
Figure 2.
Individual predictions (purple lines) and observations (yellow dots) of TS over time for five patients representing different TS profiles.

Model qualification

The good predictive performance of the final model, including dropout, was demonstrated by goodness-of-fit and VPC plots (Supplementary Figs. S1–S4). Furthermore, individual predictions described the observations well, as demonstrated for five representative patients with different tumor size profiles in **Fig. 2**.

Exploratory analysis of FcγR SNPs

All FcγR genotype categories were well represented in the data set. Of the 77 patients with MCC, for FcγRIIA, 18 had missing information, while 16, 15, and 28 had had homozygous A/A, homozygous G/G, and heterozygous A/G genotype, respectively. For FcγRIIIA, 20 patients had missing information, and 20, 14, and 23 had homozygous

Figure 3.
Spider plots of percentage tumor change from baseline versus time after the first tumor assessment in patient subgroups according to FcγRII/III genotype (FcγRIIA$_{131H}$ and FcγRIIIA$_{158V}$) in patients with mMCC. Blue lines show polynomial regression curves.

A/A, homozygous C/C, and heterozygous C/A genotype, respectively. Percentage change in TS from baseline in subgroups of patients with mMCC defined by FcγR genotype were compared (**Fig. 3**). No apparent association was found between TGD and FcγRII/III SNP. Boxplots of random parameters for CL, K_D, K_G, and the tumor shrinkage exponent decay rate λ_0 also suggested no association between FcγRII/III SNP and avelumab CL or TGD parameters (**Fig. 4**).

Bidirectional PK-TGD model

The bidirectionality of the PK-TGD model is illustrated in **Fig. 5**, which shows avelumab concentration and the percentage change of TS from baseline over time in nine simulated typical individuals differing only in initial CL and TS values.

Discussion

To our knowledge, we report the first joint PK-TGD model that characterizes the bidirectional interaction between the serum concentration of an immune checkpoint inhibitor and the corresponding TGD associated with treatment. In patients with mMCC, we observed an exposure-dependent treatment effect of avelumab in slowing down the decay of tumor shrinkage and the effect of TS on avelumab CL.

Based on a data-driven approach, in addition to the drug-induced K_D, the exposure-dependent treatment effect of avelumab was best characterized by avelumab exposure slowing the decay of tumor shrinkage, whereby higher avelumab concentrations were related to lower decay of the K_D over time (i.e., higher avelumab concentrations

reduced the drug-effect dissipation over time). This is in accordance with mechanistic expectations: by blocking the interaction between PD-1 and PD-L1, avelumab relieves T cells from immune suppression in the tumor microenvironment and prevents the loss of antitumor immunity (12), which in the model is realized through the inhibitory effect of avelumab exposure on the decay rate of tumor shrinkage over time. We did not find a significant effect of drug exposure on directly drug-induced K_D, neither exclusively nor in addition to the effect on effect decay, which might be expected from the ADCC activity of avelumab (13). This may be due to the achieved systemic exposure in the investigated population providing close to the maximum ADCC effect and, in the case of the model with the effect on both effect decay and K_D, could also be attributed to the model complexity/insufficient data and mathematical difficulty to distinguish between the two effects.

The time-varying CL of mAbs has been associated with posttreatment effects, with decreased CL observed with improved disease status and response in patients receiving treatment; this may lead to a steeper estimate of the exposure-response relationship when using the classical model with a one-way interaction between PK and PD (18, 26). Therefore, a bidirectional PK-TGD model may prevent a biased characterization of the exposure-response relationship by accounting for impact of TS on PK. As shown in **Fig. 5**, in patients with worse disease (i.e., higher initial tumor burden) but identical initial CL, lower drug concentrations were observed, thereby demonstrating the effect of TS on CL. However, despite this effect of TS, even in the patients with the highest investigated initial TS (corresponding to the 95th percentile of the empirical Bayes estimates from the final model), the
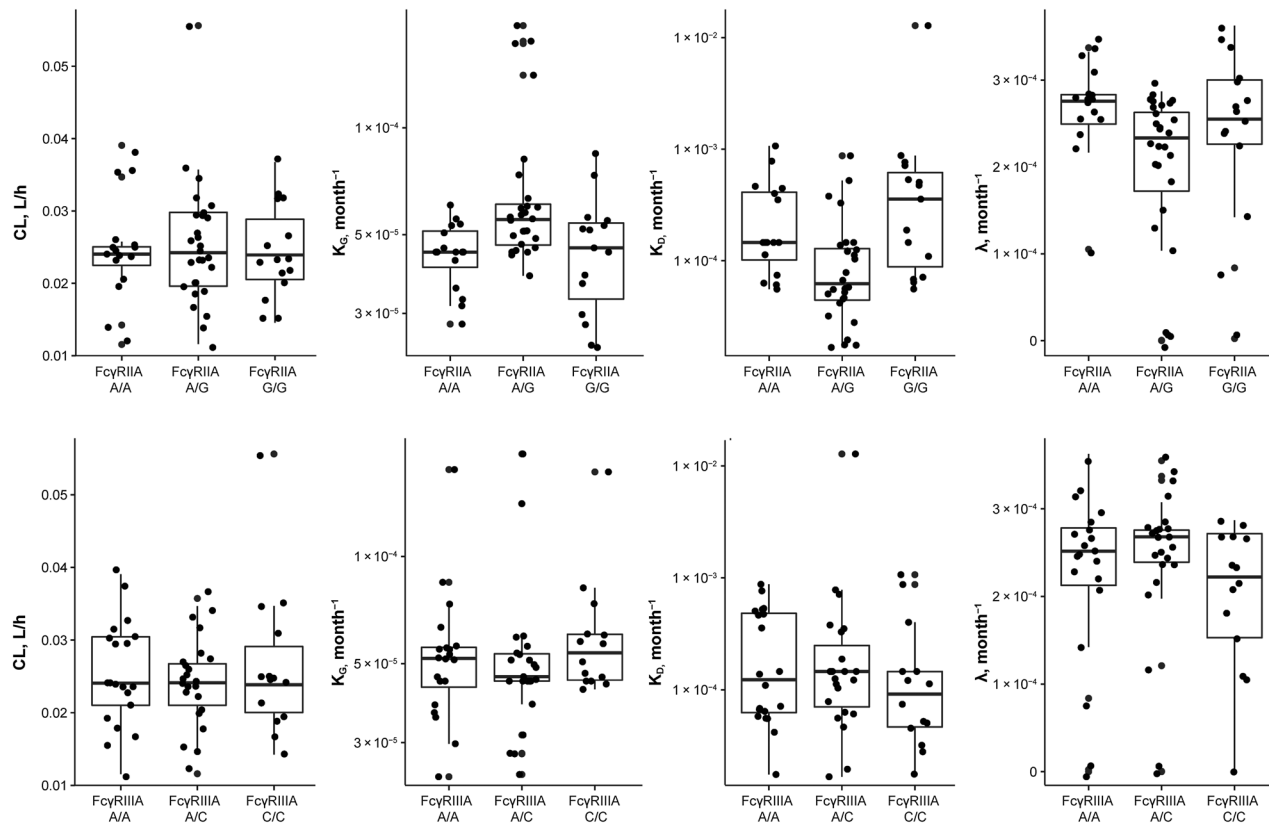
Figure 4.
Boxplots of random parameters according to FcγRII/III genotype (FcγRIIA_131H and FcγRIIIA_158V) in patients with mMCC. CL, avelumab clearance; K_D, tumor shrinkage rate; K_G, tumor growth rate; λ, decay constant of K_D.
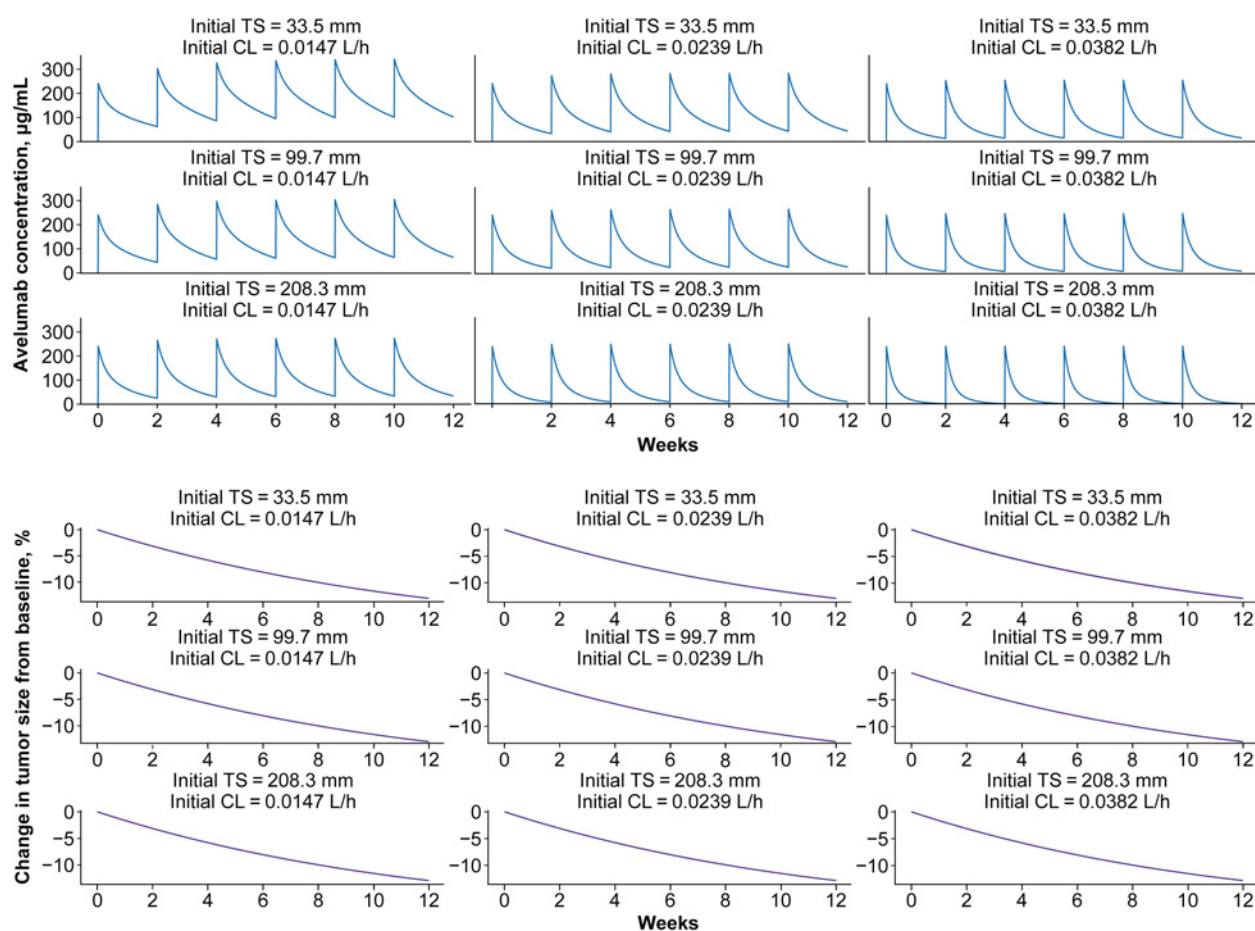
Figure 5.
Illustration of drug exposure–TS bidirectional effects via simulation of drug concentration (top panels) and percentage change of tumor size from baseline (bottom panels) over 12 weeks since first dose in 9 simulated individuals differing only in initial CL and TS. Initial CL and TS values correspond to median, and 5th and 95th percentiles of individual Bayes estimates from the final model. CL, avelumab clearance; TS, tumor size.

achieved drug exposure was shown to be sufficiently high, leading to similar tumor regression in all simulated patients (**Fig. 5**). Furthermore, while other PK parameter estimates were similar, in contrast to the initial population PK model of avelumab (17), we did not identify additional empirical time-varying CL of avelumab using the final PK-TGD model, suggesting that the changes in avelumab PK over time could be predicted by the association between longitudinal TS changes and CL. This observation is in-line with the previously reported PK-TGD model for the immune checkpoint inhibitor atezolizumab (anti–PD-L1), in which the dissipation of the treatment effect—in our model accounted for by the tumor shrinkage decay term—was addressed analogously, although it was only time dependent (27). In the atezolizumab model, tumor shrinkage was best described by cycle-specific area under the curve (AUC) rather than first-cycle AUC, despite the low level of time-varying CL for atezolizumab (27). A further PK-TGD model for the immune checkpoint inhibitor pembrolizumab (anti–PD-1) also has been published, which assumed that tumor mass has two portions, one of which is susceptible to the drug while the other is not affected by treatment (28). Similar to our model, both the atezolizumab and pembrolizumab models used modified versions of the model developed by Claret and colleagues (22, 27, 28). However, these other models accounted for the effect of drug exposure on K_D

using AUC, with atezolizumab exposure represented by individual cycle-specific AUC (27), and the effect of pembrolizumab exposure on TS analyzed through AUC over 6 weeks at steady state, which was found to be not statistically significant (28).

The model developed herein showed good performance in describing the typical PK and TS trends, but of relevance also well captured the individual TS profiles. This is demonstrated in **Fig. 2**, which shows individual predictions and observations for five representative patients who experienced different TS change trends over time: constantly increasing TS over time (patient 1), constantly decreasing TS over time (patient 2), initially decreasing TS size followed by a relapse (patient 3), initially decreasing TS reaching plateau (patient 4), and initially stagnating TS with subsequent increase (patient 5). The close overlap of individual predictions and observations in all patients demonstrates the robustness and flexibility of the model to appropriately capture different individual TS profiles.

Furthermore, by mechanistically capturing the relationship between avelumab exposure and TS, the model developed herein is expected to provide more accurate and less biased parameters, and thus enable better inferences. To investigate this, and thus the value and impact of this novel modeling approach, we compared this approach with traditional PK-TS modeling approaches in terms of

accuracy and bias of the parameter estimates, using the SSE approach. Relative RMSE and relative bias for the two compared approaches are provided in Supplementary Table S2. Both inaccuracy and bias were much lower when the bidirectionality of the PK-TS relationship was accounted for, as demonstrated by lower relative RMSE and relative bias in all (both PK- and TS-related) parameters for this model compared with the traditional PK-TS model. Because TS model–derived parameters are commonly investigated as predictors of clinical endpoints (e.g., overall survival), this would translate to those analyses as well, implying that use of the traditional model would lead to biased and potentially incorrect inferences in cases where bidirectional relationship is expected, as is the case for large molecules in oncology. The model developed herein, which accounts mechanistically for the relationship between avelumab exposure and TS by including the bidirectionality, is thereby demonstrated to reduce the bias and imprecision of such an analysis.

The potential contribution of ADCC and antibody-dependent cell phagocytosis (ADCP) to the effectiveness of immune checkpoint inhibitors is controversial. The interaction between PD-1 and PD-L1 allows ADCP and subsequent depletion of PD-1–expressing T cells, which may diminish the antitumor activity of anti–PD-1 antibodies (29). Several immune checkpoint inhibitors have been engineered to eliminate the potential for ADCC induction by IgG4 mAbs, which bind to FcγRIII with low affinity (e.g., pembrolizumab or nivolumab) or engineered IgG1 antibodies with Fc domain alterations based on the theoretical potential for depletion of T cells (e.g., atezolizumab or durvalumab; refs. 29–32). However, other evidence suggests that ADCC may enhance the antitumor effect of immune checkpoint inhibitors (33). To evaluate the potential contribution of ADCC to the clinical efficacy of avelumab, we compared tumor responses in patients of different FcγR genotypes. Specifically, SNPs within genes encoding the FcγR receptors FcγRIIIa (CD16) and FcγRIIa (CD32a), which are expressed on natural killer cells and other immunologic cells, can affect binding to the Fc region of IgG1 antibodies (34). $FcγRIIA_{131H}$ and $FcγRIIIA_{158V}$ genotypes express FcγRs with higher affinity for IgG1 and subsequently mediate greater ADCC activity than other genotypes (34). In studies of a different class of mAb, rituximab (IgG1 mAb targeted to CD20), responses were superior in patients with a high-affinity genotype ($FcγRIIIA_{158V}$) compared with those who had a low-affinity genotype ($FcγRIIIA_{158F}$; refs. 35, 36). Recent analyses in a different tumor type have suggested a potential association between FcγR alleles and survival in patients with urothelial carcinoma treated with avelumab (37). Furthermore, a recent preclinical paper (38) confirmed presence of FcγR-mediated internalization of avelumab *in vitro* and in animals. In our exploratory analyses (**Figs. 3** and **4**), we found no apparent association between FcγRIIA/IIIA SNP and TGD (K_D, K_G, nor λ) or PK (CL) in the population analyzed. Thus, we found no evidence to suggest that ADCC either increases or reduces the activity of avelumab in this population of patients with mMCC. These findings, however, do not necessarily exclude the possibility of avelumab binding to FcγR, but suggest low relevance of such potential binding. The absence of clear trends among different genotypes rather implies that, if present, the contribution of FcγR-mediated internalization to total avelumab CL and activity (ie, effect on TS) is low. Furthermore, the disagreement with previous reports might be due to potential difference between the mMCC population and urothelial carcinoma population. Another potential reason for such results might lie in the limited size of our data set, which might not have enough power to identify subtle differences among different genotypes. Of note, there were also limitations

associated with the final PK-TGD model, including the small data set for such a complex model and the limited patient follow-up time. Further external evaluations of this joint PK-TGD model are planned and have been initiated to test its applicability to different tumor types.

In conclusion, we report a semimechanistic model describing the bidirectional interaction between PK and TGD in patients with mMCC treated with second-line avelumab monotherapy, which provides mechanistic insights into the interaction between avelumab exposure and tumor growth, and may be useful for model-informed drug development of other immuno-oncology agents.

Authors' Disclosures

Authors' Contributions

A.-M. Grisic: Writing–original draft, writing–review and editing, collection and assembly of data, data analysis and interpretation, accountable for all aspects of work. **W. Xiong:** Writing–original draft, writing–review and editing, collection and assembly of data, data analysis and interpretation, accountable for all aspects of work. **L. Tanneau:** Writing–original draft, writing–review and editing, collection and assembly of data, data analysis and interpretation, accountable for all aspects of work. **S. Jönsson:** Writing–original draft, writing–review and editing, collection and assembly of data, data analysis and interpretation, accountable for all aspects of work. **L.E. Friberg:** Writing–original draft, writing–review and editing, collection and assembly of data, data analysis and interpretation, accountable for all aspects of work. **M.O. Karlsson:** Writing–original draft, writing–review and editing, collection and assembly of data, data analysis and interpretation, accountable for all aspects of work. **H. Dai:** Writing–original draft, writing–review and editing, collection and assembly of data, data analysis and interpretation, accountable for all aspects of work. **J. Zheng:** Writing–original draft, writing–review and editing, collection and assembly of data, data analysis and interpretation, accountable for all aspects of work. **P. Girard:** Writing–original draft, writing–review and editing, collection and assembly of data, data analysis and interpretation, accountable for all aspects of work. **A. Khandelwal:** Writing–original draft, writing–review and editing, collection and assembly of data, data analysis and interpretation, accountable for all aspects of work.

Acknowledgments

References

1. Tetzlaff MT, Harms PW. Danger is only skin deep: aggressive epidermal carcinomas. An overview of the diagnosis, demographics, molecular-genetics, staging, prognostic biomarkers, and therapeutic advances in Merkel cell carcinoma. Mod Pathol 2020;33:42–55.

2. NCCN Clinical Practice Guidelines in Oncology. Merkel Cell Carcinoma. v1.2021. Available from: https://www.nccn.org/professionals/physician_gls/pdf/mcc.pdf.

3. Schadendorf D, Lebbe C, Zur Hausen A, Avril MF, Hariharan S, Bharmal M, et al. Merkel cell carcinoma: Epidemiology, prognosis, therapy and unmet medical needs. Eur J Cancer 2017;71:53–69.

4. Robert C, Long GV, Brady B, Dutriaux C, Maio M, Mortier L, et al. Nivolumab in previously untreated melanoma without BRAF mutation. N Engl J Med 2015; 372:320–30.

5. Reck M, Rodriguez-Abreu D, Robinson AG, Hui R, Csoszi T, Fulop A, et al. Pembrolizumab versus chemotherapy for PD-L1-positive non-small-cell lung cancer. N Engl J Med 2016;375:1823–33.

6. Motzer RJ, Escudier B, McDermott DF, George S, Hammers HJ, Srinivas S, et al. Nivolumab versus everolimus in advanced renal-cell carcinoma. N Engl J Med 2015;373:1803–13.

7. Burtness B, Harrington KJ, Greil R, Soulieres D, Tahara M, de Castro G Jr, et al. Pembrolizumab alone or with chemotherapy versus cetuximab with chemotherapy for recurrent or metastatic squamous cell carcinoma of the head and neck (KEYNOTE-048): a randomised, open-label, phase 3 study. Lancet 2019; 394:1915–28.

8. Bellmunt J, de Wit R, Vaughn DJ, Fradet Y, Lee JL, Fong L, et al. Pembrolizumab as second-line therapy for advanced urothelial carcinoma. N Engl J Med 2017; 376:1015–26.

9. Kaufman HL, Russell J, Hamid O, Bhatia S, Terheyden P, D'Angelo SP, et al. Avelumab in patients with chemotherapy-refractory metastatic Merkel cell carcinoma: a multicentre, single-group, open-label, phase 2 trial. Lancet Oncol 2016;17:1374–85.

10. Bavencio (avelumab). Prescribing information. EMD Serono; 2020.

11. Bavencio (avelumab). Summary of product characteristics. Merck KGaA, Darmstadt, Germany; 2021.

12. Heery CR, O'Sullivan-Coyne G, Madan RA, Cordes L, Rajan A, Rauckhorst M, et al. Avelumab for metastatic or locally advanced previously treated solid tumours (JAVELIN Solid Tumor): a phase 1a, multicohort, dose-escalation trial. Lancet Oncol 2017;18:587–98.

13. Boyerinas B, Jochems C, Fantini M, Heery CR, Gulley JL, Tsang KY, et al. Antibody-dependent cellular cytotoxicity activity of a novel anti-PD-L1 antibody avelumab (MSB0010718C) on human tumor cells. Cancer Immunol Res 2015;3:1148–57.

14. Lobo ED, Hansen RJ, Balthasar JP. Antibody pharmacokinetics and pharmacodynamics. J Pharm Sci 2004;93:2645–68.

15. Ryman JT, Meibohm B. Pharmacokinetics of monoclonal antibodies. CPT Pharmacometrics Syst Pharmacol 2017;6:576–88.

16. Centanni M, Moes DJAR, Trocóniz IF, Ciccolini J, van Hasselt JGC. Clinical pharmacokinetics and pharmacodynamics of immune checkpoint inhibitors. Clin Pharmacokinet 2019;58:835–57.

17. Wilkins JJ, Brockhaus B, Dai H, Vugmeyster Y, White JT, Brar S, et al. Time-varying clearance and impact of disease state on the pharmacokinetics of avelumab in Merkel cell carcinoma and urothelial carcinoma. CPT Pharmacometrics Syst Pharmacol 2019;8:415–27.

18. Liu C, Yu J, Li H, Liu J, Xu Y, Song P, et al. Association of time-varying clearance of nivolumab with disease dynamics and its implications on exposure response analysis. Clin Pharmacol Ther 2017;101:657–66.

19. Li H, Yu J, Liu C, Liu J, Subramaniam S, Zhao H, et al. Time dependent pharmacokinetics of pembrolizumab in patients with solid tumor and its correlation with best overall response. J Pharmacokinet Pharmacodyn 2017; 44:403–14.

20. Doi T, Iwasa S, Muro K, Satoh T, Hironaka S, Esaki T, et al. Phase 1 trial of avelumab (anti-PD-L1) in Japanese patients with advanced solid tumors,

21. including dose expansion in patients with gastric or gastroesophageal junction cancer: the JAVELIN Solid Tumor JPN trial. Gastric Cancer 2019;22: 817–27.

21. BLA Multidisciplinary Review and Evaluation: BLA 761049 Bavencio (Avelumab). 2017. Avaialble from: https://www.accessdata.fda.gov/drugsatfda_docs/nda/2017/761049Orig1s000MultidisciplineR.pdf.

22. Claret L, Girard P, Hoff PM, Van Cutsem E, Zuideveld KP, Jorga K, et al. Model-based prediction of phase III overall survival in colorectal cancer on the basis of phase II tumor dynamics. J Clin Oncol 2009;27:4103–8.

23. Nordgren R, Ueckert S, Yngman G, Assawasuwannakit P, Hooker AC, Karlsson MO. Perl speaks NONMEM (PsN). Abstract 9095. Presented at: PAGE 2019, Stockholm, Sweden. 2019.

24. Friberg LE, de Greef R, Kerbusch T, Karlsson MO. Modeling and simulation of the time course of asenapine exposure response and dropout patterns in acute schizophrenia. Clin Pharmacol Ther 2009;86:84–91.

25. Eisenhauer EA, Therasse P, Bogaerts J, Schwartz LH, Sargent D, Ford R, et al. New response evaluation criteria in solid tumours: revised RECIST guideline (version 1.1). Eur J Cancer 2009;45:228–47.

26. Grisic A-M, Khandelwal A, Bertolino M, Huisinga W, Girard P, Kloft C. Semimechanistic clearance models of oncology biotherapeutics and impact of study design: cetuximab as a case study. CPT Pharmacometrics Syst Pharmacol 2020;9:628–38.

27. Netterberg I, Li CC, Molinero L, Budha N, Sukumaran S, Stroh M, et al. A PK/PD analysis of circulating biomarkers and their relationship to tumor response in atezolizumab-treated non-small cell lung cancer patients. Clin Pharmacol Ther 2019;105:486–95.

28. Chatterjee MS, Elassaiss-Schaap J, Lindauer A, Turner DC, Sostelly A, Freshwater T, et al. Population pharmacokinetic/pharmacodynamic modeling of tumor size dynamics in pembrolizumab-treated advanced melanoma. CPT Pharmacometrics Syst Pharmacol 2017;6:29–39.

29. Zhang T, Song X, Xu L, Ma J, Zhang Y, Gong W, et al. The binding of an anti-PD-1 antibody to FcγRI has a profound impact on its biological functions. Cancer Immunol Immunother 2018;67:1079–90.

30. Powles T, Eder JP, Fine GD, Braiteh FS, Loriot Y, Cruz C, et al. MPDL3280A (anti-PD-L1) treatment leads to clinical activity in metastatic bladder cancer. Nature 2014;515:558–62.

31. Herbst RS, Soria JC, Kowanetz M, Fine GD, Hamid O, Gordon MS, et al. Predictive correlates of response to the anti-PD-L1 antibody MPDL3280A in cancer patients. Nature 2014;515:563–7.

32. Chen X, Song X, Li K, Zhang T. FcγR-binding is an important functional attribute for immune checkpoint antibodies in cancer immunotherapy. Front Immunol 2019;10:292.

33. Clynes RA, Towers TL, Presta LG, Ravetch JV. Inhibitory Fc receptors modulate in vivo cytotoxicity against tumor targets. Nat Med 2000;6:443–6.

34. Bruhns P, Iannascoli B, England P, Mancardi DA, Fernandez N, Jorieux S, et al. Specificity and affinity of human Fcγ receptors and their polymorphic variants for human IgG subclasses. Blood 2009;113:3716–25.

35. Cartron G, Dacheux L, Salles G, Solal-Celigny P, Bardos P, Colombat P, et al. Therapeutic activity of humanized anti-CD20 monoclonal antibody and polymorphism in IgG Fc receptor FcgammaRIIIa gene. Blood 2002;99: 754–8.

36. Weng WK, Levy R. Two immunoglobulin G fragment C receptor polymorphisms independently predict response to rituximab in patients with follicular lymphoma. J Clin Oncol 2003;21:3940–7.

37. Powles TB, Loriot Y, Bellmunt J, Sternberg CN, Sridhar S, Petrylak DP, et al. 699O Avelumab first-line (1L) maintenance + best supportive care (BSC) vs BSC alone for advanced urothelial carcinoma (UC): Association between clinical outcomes and exploratory biomarkers. Ann Oncol 2020;31:S552–S3.

38. Jin H, D'Urso V, Neuteboom B, McKenna SD, Schweickhardt R, Gross AW, et al. Avelumab internalization by human circulating immune cells is mediated by both Fc gamma receptor and PD-L1 binding. Oncoimmunology 2021;10: 1958590.